Name: Lavleen Bhat
Student Number: 17210637
Email ID: Lavleen.bhat2@mail.dcu.ie
Programme: Master's in computing (Data Analytics)
Module Code: CA685
Date: 10/08/2018

Disclaimer:

A report submitted to Dublin City University, School of Computing for module CA685 Data Analytics Practicum, 2017/2018.

I understand that the University regards breaches of academic integrity and plagiarism as grave and serious.

I have read and understood the DCU Academic Integrity and Plagiarism Policy. I accept the penalties that may be imposed should I engage in practice or practices that breach this policy.

I have identified and included the source of all facts, ideas, opinions, viewpoints of others in the assignment references. Direct quotations, paraphrasing, discussion of ideas from books, journal articles, internet sources, module text, or any other source whatsoever are acknowledged, and the sources cited are identified in the assignment references.

I declare that this material, which I now submit for assessment, is entirely my own work and has not been taken from the work of others save and to the extent that such work has been cited and acknowledged within the text of my work.

By signing this form or by submitting this material online I confirm that this assignment, or any part of it, has not been previously submitted by me or any other person for assessment on this or any other course of study. By signing this form or by submitting material for assessment online I confirm that I have read and understood DCU Academic Integrity and Plagiarism Policy (available at: http://www.dcu.ie/registry/examinations/index.shtml)

Name(s): Lavleen Bhat
Date: 10/08/2018

Lung Nodule Detection using Deep Convolutional Neural Networks

Lavleen Bhat
School of Computing, Dublin City University, Ireland
Email: lavleen.bhat2@mail.dcu.ie

***Abstract*—Pulmonary lung cancer is the leading cause of cancer related deaths worldwide. To detect the cancer at an early stage is the key to early diagnosis and timely treatment. Projecting high risk cancer patients to low-dose CT scans have resulted in 20% less mortality rates. Reading these low-dose CT scans can be a cumbersome task for radiologists and hence a good Computer Aided Detection (CAD) is required in place to assist the radiologists. Computer Aided cancer detection can be divided into two main parts: nodule detection and nodule malignancy classification. In this paper, we cover the first part of cancer detection and present a CAD system with the aim to localise as many nodules as possible with least false positive rate. The system uses a Faster R-CNN region proposal network based structure to identify and predict the nodules regions and is evaluated on a standard dataset allowing comparison with the work of others.**

Keywords - Lung Nodule Detection, Region Proposal Network, Deep learning, 3D CNN

I. Introduction

Latest studies have shown that there is a drop in the rate of mortality when high-risk lung cancer patients are subjected to low-dose CT scan technology as compared to chest radiography. High-risk lung cancer patients include people ranging from the age of 55 to 80 and who have a history of smoking. Only high-risk patients are seen to benefit from the low dose CT scan technology as it does not have much impact on individuals having a healthy lifestyle along with smoking. So, the U.S. Preventive Services Task Force (USPSTF) has given low dose CT scans a B-grade recommendation [19].

Early detection (Stage 1A – Nodules $< 3cm$) of lung cancer paves a way for early diagnosis and increases the chances of survival which drop drastically if the patient has reached stage 1B (nodules $> 3cm$). A lot of research has been done and is still ongoing in this area of medical science. Computer aided diagnosis is needed to control and prevent the slightest error in detection of nodules which will directly impact the rate of mortality in case of lung disease. CAD systems can thus assist experienced radiologists to detect the lung cancer at early stages which will help in early and effective diagnosis of patients.

Medical imaging analysis is very different from other computer vision applications. The most popular computer vision problems involve analysing 2D images mostly while this is not the case in medical imaging analysis. Medical images are 3D in nature and have multiple types of formats (e.g. .MHD, .DCM) which have multiple 2D images in them that combine and make up the full 3D image. Object detection in 3D images have the largest difficulty because most of these require much computing resources and in recent times this has been Graphical Processing Unites (GPUs) but there is limited GPU memory available. We cannot use the already available models trained on 2D images like ImageNet [14] etc. for this task simply because the objects to be localised are different than the data these models are trained on. The nodules in lung tissue can have varying shape and size. They're completely different from day-to-day objects.

So, keeping these differences and difficulties in mind, the system presented in this paper proposes the 3D region of interest for all the possible nodules in the images. The system uses a 3D CNN to extract the features and learn to identify the suspected nodule regions.

A. Motivation

In 2016, the LUNA-16 open grand challenge [3] was organised to develop a state-of-the-art CAD system to detect cancerous lung nodules from 3D images, with highest accuracy. The data-set was picked from the LIDC/IDRI public medical imaging database.

In May 2017, Kaggle [2], the online machine learning website, held a similar competition to develop a CAD system for the same purpose. Kaggle used a different data-set than LUNA-16. The file format used in the LUNA-16 challenge was RAW CT scans while the Kaggle data-set included DICOM format CT scans [8].

The system in this paper is trained on the same data-set as in LUNA-16 i.e., the LIDC/IDRI data-set which includes 888 low-dose CT scans with manual annotations for the presence of lung nodules from 4 experienced radiologists.

B. Paper Structure

The rest of this paper is divided into five parts: Section II contains the literature review of automatic lung nodule detection. Section III includes the approach used to tackle the problem and build the CAD system, Section IV includes the experimental setup and the results, Section V presents the conclusion, and finally Section VI presents future work on the problem.

II. Literature Review

The published literature for object detection is vast. Most of the object detection in computer vision is done on 2D

images. To adapt any of these state-of-the-art models for 3D object detection, the 2D models are run on individual 2D images and then combine the results to make 3D object detection.

Until 2017, almost all the research on lung nodule detection was based on 2D input data only. CT scans are generally 3D in shape consisting of multiple 2D slices and resulting in a 3D scan after combining those slices. The models developed for this purpose based on 2D processing achieved a significant level of accuracy and sensitivity. But making use of 3D nature of the nodules and using features such as viscosity and shape of the nodules can improve the results even further.

In [19], the author explains different techniques used for object identification. Active Shape Models(ASM), Active Appearance Models (AAM) and Active Tensor Models (ATM) are combined along with template matching for energy optimization. The model works mainly upon two-dimensional images to identify lung nodules less than 1cm in diameter, which is not very efficient as the Low-dose CT scans are three-dimensional.

In [12], the authors describe an algorithm used for nodule detection in low-dose CT scan images on a large-scale evaluation. The authors used a local image feature algorithm to identify the nodule shape and two successive k-nearest-neighbour classifications to reduce false-positives.

In [5] the authors describes a CAD system built in the C# language for automatic detection of lung nodules. The system is designed on a data-driven framework. The author describes segmentation techniques like AAM and ASM used for detection of the nodule and modeling the CAD system.

Deep learning based CAD systems started pouring in after Kai et al pusblished their first research on comparison of conventional CAD systems and Deep Belief Network and convolutional neural network based models. [11] The authors showed how deep learning based CAD models can achieve better results than conventional CAD systems by feature extraction. Paper also highlights that the models are baseline models and there's a scope of extending this research further by incorporating input data images size cue which they could not study.

Working on LIDC-IDRI dataset, the authors of [7] achieved high detection sensitivities of 85.4% and 90.1% at 1 and 4 false positives per scan, respectively. The authors make use of 2D conv nets for both detection and classification tasks. In other similar research [18], the authors use an off-the-shelf network OverFeat trained on normal images and then they apply it on the lung cancer detection task.

In [1], the authors talk about the application of deep convolutional networks on 2D and 2.5D images of lung scans. The authors designed a two-tier CAD system in which the coordinates of the region of interest are generated in the first tier and fed to the second tier as input. This way the system is trained on deep convolutional neural network and generated the highest accuracy of 77%.

In the most recent published methods, [9], [10], [15], the participants of LUNA-16 competition achieved the highest sensitivity and accuracy between 94% and 95% by training and using 3D convolutional neural networks. The winners of the evaluation [15], trained a 3D CNN for detection of nodules and two 3D CNNs for reducing false positives and classifying the nodules. The authors used a new focal loss function to deal with unbalanced classification and batch and weight normalisation to obtain better final results.

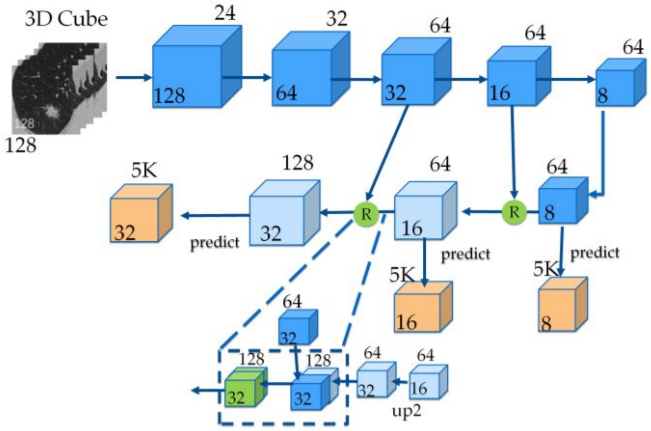

Figure 1. Architecture of DSB & LUNA winning models

In [10], the authors used a two-stage nodule detection framework where one CNN is trained separately on 2D axial slices and 3D volume. For classification, authors trained a 3D residual network to achieve a final FROC score of 94.99%.

In a parallel evaluation competition held by Kaggle in 2017, the winners [8] of the competition propose a two stage 3D deep neural network cancer detection model where the first stage for nodule detection is based on the Faster R-CNN's region proposal network. The second stage takes the top five region proposals and assigns the malignant probability by using a leaky noisy-or gate.

The winners of both the competitions [8] and [15] have similar architecture shown in Figure 1.

III. APPROACH

There are many pre-trained networks available for computer vision problems like ImageNet, VGG-16 Net etc. They all use and work on 2D data consisting of natural images and are difficult to adapt for 3D medical data. These are the two main reasons for not starting the project with pre-trained networks. First, being the 3D nature of the data and second that these networks are built to detect general multi-class objects. Adapting them to single class object detection in medical imaging data is the same as building a new network and training it on medical image data.

The proposed pipeline for this project shown in Figure 2, takes the 3D CT scans as input. The raw images contain a lot

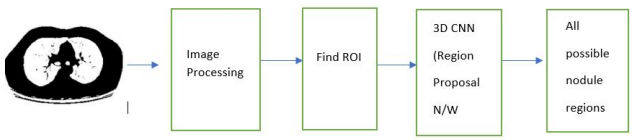

Figure 2. Pipeline of proposed CAD system

of noise and hence image pre-processing is necessary. After pre-processing the image and taking out only the required lungs area after removing the noise from the volumetric images, data is fed to next layer to mark the region of interest. Regions of interest in our case are the potential lung nodules. After detecting the regions of interest, a 3D Deep CNN is trained to propose regions with inputs as the original CT scan and nodule masks created in previous step.

A. *Data Understanding*

The data we use in our experiments consists of 888 low dose CT scans. The scans are in RAW (.MHD) file format. Each CT scan has two files associated with it where one file contains the metadata and other the actual pixel values. Given the nature of the data being 3 dimensional, the files are huge in size with 500 MB in each image. Total data is 62 GB in compressed format.

To handle such large data, a HDF5 file server was setup where images are stored in a compressed format using GZIP. HDF5 enables storage of large numpy values with unlimited storage. This server is used to store intermediate results such as nodule masks as well.

B. *Data Preprocessing*

The first and most crucial step of any machine learning project is the data cleaning and pre-processing. To pre-process images in this application, the task was divided into the following stages:

*1) **Image resizing**:* Number of slices and the spacing depends on how the CT scan machine is calibrated. The scans in the current dataset do not have a constant spacing in any dimension. The spacing on the Z-axis varies between 0.625 mm to 2.5 mm and the same on X- and Y-axes. This can cause issues during training of neural networks which requires the input size to be the same and consistent. Hence, the dimensions of each image are factored by to 1mm * 1mm * 1mm spacing.

Few of the image slices at both the ends of the lungs cannot have nodules because of the irregular shape of the nodules and hence 15 slices from each end are removed before processing the images further. So, only the larger areas of the lungs are scanned for nodules. This step results in reduction in the size of the input image by approximately $1/4^{th}$ of the number of slices.

*2) **Image Segmentation**:* The nodules to be detected are present in the lung area and because the shape of the nodules can be spherical, other body parts captured in the CT scan having spherical shapes can be inadvertently considered as nodules. To rule out such errors, the area outside lungs should be removed. The potential nodules could be attached to the walls of the lungs and hence to carefully extract only the lung area from CT scans, we go through the following steps:

(i) Binary conversion: The CT scan images do not have RGB channels and are already gray-scaled. Before further processing, the images are converted to binary images. The standard unit for measuring radiodensity is Hounsfield Unit (HU) and this unit can be used for thresholding the images. There are different HU values for each kind of tissue inside the lungs and it is same for every patient. It was found in experiments [16] that the threshold value of 604 can be successfully used for segmenting the lung area from the rest of the body.

(ii) Noise Removal: During data processing it was noticed that some of the images had salt and pepper noise. The most effective method to remove salt and pepper noise is to use a technique called Median Blur [17]. This method takes the median value of all the pixels under the kernel area and replaces the central pixel value with that median value.

(iii) Morphological Operations: Next, to remove the noise from the area outside lung regions, the OPENING operation is performed. The opening operation is just another name for Erosion followed by Dilation. This operation removes the small blobs outside the lung area and near the boundary of the image.

Now, to remove the noise and fill the small holes inside the lungs area, the CLOSING operation is performed. This operation removes the noise inside the lung region and we get a uniform lung region to be segmented further. The Closing operation is just the opposite of Opening — dilation followed by erosion.

Erosion operation converts the pixels underlying the kernel to 1 if all the pixels under that kernel are 1. Dilation operation does the exact opposite. If at least one pixel under the kernel is 1, the pixel elements will be converted to 1. So, erosion shrinks the white region and dilation increases it.

(iv) Clear border and label: After all the noise has been removed from the image, the image areas are labelled for final segmentation of lung regions. Other algorithms such as the watershed algorithm [20] was also tried to segment the lung areas but this simple method gives better results.

(v) Segmentation: After labelling the image in previous step, the two largest areas from the images are kept. These two largest areas are the lung areas. Thus, lungs are segmented from original image by creating a lung mask.

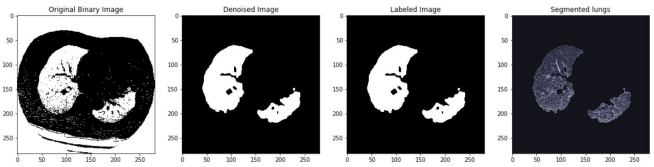

Figure 3. Segmented Lungs after noise removal

Once we get the lung mask containing only the lungs area as the white region, it is overlapped with the original image to segment out the lungs ignoring the non-ROI regions.

Figure 3 depicts the whole operation of image pre-processing. The slice shown in the figure contains salt and pepper noise and we are able to get almost complete region of the lungs area after image pre-processing steps explained.

*3) **Data Augmentation**:* There is a class imbalance between positive and negative cancer cases. This imbalance might result in overfitting and biasing. To handle this, the data is synthetically generated using common data augmentation methods. In data augmentation, operations such as flipping and rotating image to 90, 180, and 270 degrees, zoom in and zoom out, have been applied.

C. Marking Region of Interest (ROI)

To narrow our search region, we have already isolated the lung regions from the rest of the area in the image with preserved edges of the lungs so we do not miss the nodules near the walls of the lungs.

Now, to localise the nodules that are our region of interest in the segmented lung region, annotations provided in the dataset by the radiologist are used. The annotations file has the annotations from 4 experienced radiologists with their X, Y, Z coordinates and the diameter of the nodule. There are a total of 1187 malignant nodules annotated in the whole dataset. The nodules in the annotations are provided as the spherical nodules with the diameter of each nodule. This data is utilised to take out the nodule regions.

To mark the nodule areas and draw the circles around nodules, nodule range is determined by using the radius of the annotated nodules. The pixels in this determined nodule range are set to 1 and rest of the area pixels are set to 0. This way, a binary mask is prepared containing only the nodule region. The nodule masks are obtained from segmented lungs from previous step, and not from original images because we're interested in only lung area.

D. Region Proposal Network

Region proposal network takes the inspiration from Faster R-CNN utilising only Region Proposal Network part. Classification part of Faster R-CNN is not considered since there are only two classes of objects – nodule and rest of the region. The architecture of the region proposal network is based on U-net used for biomedical images segmentation [13].

*1) **Architecture**:* The architecture of the 3D deep convolutional neural network is based on the U-Net model. The U-net model was introduced in 2015 with an aim to train the deep neural networks with very few data. Conventional deep convolutional neural networks were limited by the size of the data required to train a neural network end-to-end and the size of the network itself.

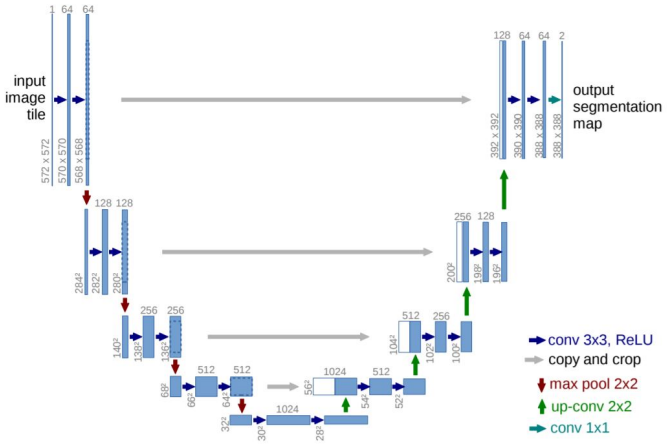

Figure 4. Architecture of U-net model

U-net model proved to be a groundbreaking study because it can be trained on very few training dataset and yields more precise segmentations than conventional deep networks. Figure 4 shows the network architecture consisting of contracting parts on the left and upsampling parts on the right. The contracting part consists of two normal 3*3 convolutions followed by a 2*2 max-pooling layer in each step. The activation used for convolution layers is rectified linear unit (ReLU). At each downsampling step the number of feature channels are doubled. Coming to the upsampling part on the right, each upsampling layer in every step is a 2*2 convolutional layer that halves the feature channels, followed by two 3*3 convolutional layers. After upsampling by 2*2 convolutions, layer is merged with the corresponding layer on the downsampling part and after concatenation only 3*3 convolutions are added. At the final layer, a 1*1 convolution is added to get the proposals. The original model has 23 convolutional layers in total.

The model used in this paper has a total of 19 layers following the same architecture. The proposed model is the 3D adaptation of the 2D U-net model explained above. The layers in the contracting path in original Unet model use dropout layers to perform implicit data augmentations and to avoid overfitting. The proposed model replaces the dropout layers with batch normalization layers. The drop out layers are used at the time of upsampling after the concatenation. This way the data is normalized without any need of normalizing it explicitly and overfitting is avoided by using drop out layers near the end of the convolution model.

Layer (type)	Output Shape	Param #	Connected to
input_1 (InputLayer)	(None, 1, 512, 512,	0	
conv3d_1 (Conv3D)	(None, 1, 512, 512,	432064	input_1[0][0]
conv3d_2 (Conv3D)	(None, 1, 512, 512,	110656	conv3d_1[0][0]
max_pooling3d_1 (MaxPooling3D)	(None, 1, 256, 256,	0	conv3d_2[0][0]
conv3d_3 (Conv3D)	(None, 1, 256, 256,	110720	max_pooling3d_1[0][0]
conv3d_4 (Conv3D)	(None, 1, 256, 256,	442496	conv3d_3[0][0]
max_pooling3d_2 (MaxPooling3D)	(None, 1, 128, 128,	0	conv3d_4[0][0]
conv3d_5 (Conv3D)	(None, 1, 128, 128,	442624	max_pooling3d_2[0][0]
conv3d_6 (Conv3D)	(None, 1, 128, 128,	442432	conv3d_5[0][0]
up_sampling3d_1 (UpSampling3D)	(None, 1, 256, 256,	0	conv3d_6[0][0]
concatenate_1 (Concatenate)	(None, 2, 256, 256,	0	up_sampling3d_1[0][0] conv3d_4[0][0]
conv3d_7 (Conv3D)	(None, 2, 256, 256,	442496	concatenate_1[0][0]
dropout_1 (Dropout)	(None, 2, 256, 256,	0	conv3d_7[0][0]
conv3d_8 (Conv3D)	(None, 2, 256, 256,	110624	dropout_1[0][0]
up_sampling3d_2 (UpSampling3D)	(None, 2, 512, 512,	0	conv3d_8[0][0]
concatenate_2 (Concatenate)	(None, 3, 512, 512,	0	up_sampling3d_2[0][0] conv3d_2[0][0]
conv3d_9 (Conv3D)	(None, 3, 512, 512,	110656	concatenate_2[0][0]
dropout_2 (Dropout)	(None, 3, 512, 512,	0	conv3d_9[0][0]
conv3d_10 (Conv3D)	(None, 3, 512, 512,	110656	dropout_2[0][0]
conv3d_11 (Conv3D)	(None, 3, 512, 512,	65	conv3d_10[0][0]

Total params: 2,755,489
Trainable params: 2,755,489
Non-trainable params: 0

Figure 5. Summary of the desgined 3D convolutional network

Figure 5 shows the summary of the 3D region proposal network designed. The network is divided into five total steps. First step (Step 1) contains two convolution layers combined with the max pool layer. Max pool layer reduces the size of input by half with a filter of size 2*2*2. The number of filters used in first layer are 64. So, the output shape from first set of convolution layers is 64*512*512. Next step (Step 2) contains the same layers and reduces the size of the input further by half and outputs a shape of 128*128*128 after passing through max pool layer. In the next step (Step 3), another two convolution layers are added giving the output shape of 64*128*128.

Now, in the backward pass, expansion of the layers is started. The output from the previous layer is upsampled and concatenated with the corresponding downsampling layer from step 2. Here, a dropout layer is used to avoid overfitting. After adding another layer of convolution, next step uses this output and upsamples the input. This upsampling output is concatenated with corresponding downsampling Step 1 layer output. The final layer consists of 1*1 filter for final region proposals. The final output layer generates the region proposal in the original shape of 512*512.

The number of total and trainable parameters generated in the neural network are 2,755,489.

IV. Experimental Setup and Results

A. Training and Testing

The model has been trained on NVIDIA GTX 660 Ti GPU. The model takes the segmented lung images as the training input and the nodule masks prepared in ROI section as the ground truth. The data was divided into 70:30 ratio for training and testing data. So, the model was trained on 623 images and tested on rest of the 265 images.

To fully utilise the GPU memory, the full size images are used as input and batch size is kept at 1. The input images are padded so that the size of the images is maintained.

*1) **Loss Function**:* The evaluation of the model is done by the Dice coefficient function [4]. Dice coefficient function can very well handle the class imbalance in the segmentation and that is the reason to use this loss function here. There will be class imbalance in the dataset which might results in overfitting and thouhg other methods of handling overfitting have been used, dice coefficient function can precisely describe the predictions accuracy. The formula used to calculate the loss is as follow:

$$\mathrm{DL}_2 = 1 - \frac{\sum_{n=1}^{N} p_n r_n + \epsilon}{\sum_{n=1}^{N} p_n + r_n + \epsilon} - \frac{\sum_{n=1}^{N} (1-p_n)(1-r_n) + \epsilon}{\sum_{n=1}^{N} 2 - p_n - r_n + \epsilon}$$

The dice coefficient measures the similarity between the target and the predicted output and gives a score between 0 and 1 depending on the similarity. If all the elements between the target and predicted result match, the output score is 1. If no elements match, the output score is set to 0. And the score will be between 0 and 1 if there is some percentage of similarity between them.

*2) **Optimization**:* The optimization algorithm used for the learning rate is Adam [6]. Adam is a recently introduced computationally efficient optimization algorithm which performs better than classical algorithms such as stochastic gradient descent (SGD). Adam algorithm combines the benefits of both the other extension optimization algorithms of SGD – AdaGrad and RMSProp. Unlike these methods, Adam optimization algorithm calculates the exponential moving average of the gradient and the squared gradient. The optimizer in the model was started with the initial learning rate of 0.0001.

*3) **Activation**:* The model uses Rectified Linear unit (ReLU) for activating the network layers. ReLU function gives the major advantage of reduced likelihood of vanishing gradients over Sigmoid activations. This results in faster learning of the model by keeping the gradients constants. Another advantage of using ReLU is that the networks convergence performance is better than sigmoid activations.

B. Results

Figure 6 shows the example of a nodule inside one of the slices in the CT scan on left and the right image is the mask generated by marking region of interest. The results of the neural network predicts such masks and when appended with the original image, suspicious nodules in the lungs are found. The final loss using the dice coefficient function predicted on the dataset is -0.2811.

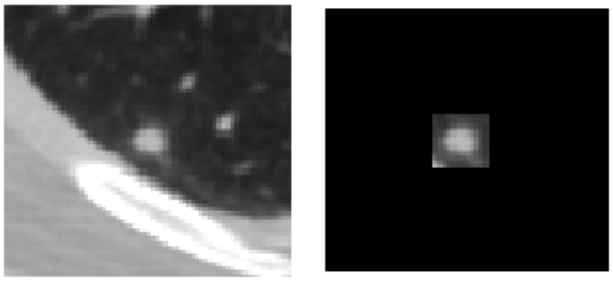

Figure 6. Example of predicted nodule mask

C. *Results*

Training:

	TRAINING	
	Model 1 (23 layers)	**Model 2 (19 layers)**
DICE COEFFICIENT LOSS	**-0.3202**	**-0.2872**
AUC SCORE	**0.6915**	**0.7155**

Testing:

	TESTING	
	Model 1 (23 layers)	**Model 2 (19 layers)**
DICE COEFFICIENT LOSS	**-0.2978**	**-0.2811**
AUC SCORE	**0.6790**	**0.6843**

V. Conclusion

CAD systems have been used for decades in the field of medical science. With the recent advancements in technology, medical science has got more specialised. Effective treatment of the patients majorly depends on the early detection of the disease. Early detection gives a path for early and effective treatment. Accurate detection of the disease and in our case accurate detection of the pulmonary lung nodules can prove to be significant for the screening and treatment on large scale. This paper describes the design of such CAD system that can help in large scale screening of low dose CT scans and pave a way for early detection and treatment of lung disease.

VI. Future Work

The model proposed in the paper detects all the suspicious lung nodules with highest possible accuracy. The model can be easily extended to help with cancer classification task. The model gives out all the region proposal for the lung nodules and these lung nodules can be used as input to another convolution network to classify the probability of nodule being malignant or benign.

Acknowledgements

The model was trained on a NVIDIA GTX 660 Ti GPU made available by my supervisor Alan Smeaton, Founding Director of the Insight Centre for Data Analytics at DCU.

References

[1] Convolutional neural networks. https://en.wikipedia.org/wiki/Convolutional_neural_network. Accessed: 14 February, 2018.

[2] Data science bowl 2017. https://www.kaggle.com/c/data-science-bowl-2017. Accessed: 14 February, 2018.

[3] Lung nodule analysis 2016. https://luna16.grand-challenge.org/home/. Accessed: 14 February, 2018.

[4] Tom Vercauteren Sebastien Ourselin Carole H. Sudre, Wenqi Li and M. Jorge Cardoso. Generalised dice overlap as a deep learning loss function for highly unbalanced segmentations. 2017.

[5] Cambron N Carter. *CAD system for lung nodule analysis*. University of Louisville, 2013.

[6] Jimmy Lei Ba Diederik P. Kingma. Adam: A method for stochastic optimization. 2015.

[7] Arnaud Arindra Adiyoso Setio et al. Pulmonary nodule detection in ct images: False positive reduction using multi-view convolutional networks. 2016.

[8] Zhe Li Xiaolin Hu* Senior Member Fangzhou Liao, Ming Liang. Evaluate the malignancy of pulmonary nodules using the 3d deep leaky noisy-or network. 2017.

[9] Fonova. 3d deep convolution neural network application in lung nodule detection on ct images. 2017.

[10] Han Yang Hongli Ji Linyang He Haiqi Xia Yadong Zhou Guohua Cheng, Weiyi Xie. Deep convolution neural networks for pulmonary nodule detection in ct imaging. 2017.

[11] Shintami Chusnul Hidayati Wen-Huang Cheng Kai-Lung Hua, Che-Hao Hsu and Yu-Jen Chen. Computer-aided classification of lung nodules on computed tomography images via deep learning technique. 2015.

[12] Keelin Murphy, Bram van Ginneken, Arnold MR Schilham, BJ De Hoop, HA Gietema, and Mathias Prokop. A large-scale evaluation of automatic pulmonary nodule detection in chest ct using local image features and k-nearest-neighbour classification. *Medical image analysis*, 13(5):757–770, 2009.

[13] Philipp Fischer Olaf Ronneberger and Thomas Brox. U-net: Convolutional networks for biomedical image segmentation. 2015.

[14] Hao Su Jonathan Krause Sanjeev Satheesh-Sean Ma Zhiheng Huang Andrej Karpathy Aditya Khosla Michael Bernstein Alexander C. Berg Li Fei-Fei Olga Russakovsky, Jia Deng. Imagenet large scale visual recognition challenge. 2015.

[15] China Ping An Technology (Shenzhen) Co., Ltd. 3dcnn for lung nodule detection and false positive reduction. 2018.

[16] Ravi Shankar M Bhaskar Rao N Sasidhar B, Ramesh Babu D R. Automated segmentation of lung regions using morphological operators in ct scan. 2013.

[17] Sin Hoong Teoh and Haidi Ibrahim. Median filtering frameworks for reducing impulse noise from grayscale digital images: A literature survey. 2012.

[18] Bram van Ginneken ; Arnaud A. A. Setio ; Colin Jacobs ; Francesco Ciompi. Off-the-shelf convolutional neural network features for pulmonary nodule detection in computed tomography scans. 2015.

[19] MPH Virginia A. Moyer, MD. Screening for lung cancer: U.s. preventive services task force recommendation statement. 2014.

[20] Guowei Yang Shaolong Wu Xuemei Cui, Yan Deng. An improved image segmentation algorithm based on the watershed transform. 2014.